Aluminum oxide barrier coatings on polymer films for food packaging applications

C. F. Struller[a, b], P. J. Kelly[a], N. J. Copeland[b]

[a]Surface Engineering Group, Manchester Metropolitan University, Manchester, M1 5GD, UK

[b]Bobst Manchester Ltd., Pilsworth Road, Heywood, Lancashire OL10 2TL, UK

Corresponding author: Carolin Struller

Telephone: +44 (0)75 99404360

Fax: +44 (0)161 247 4693

E-mail: carolin.struller@stu.mmu.ac.uk

ABSTRACT

In the field of packaging, barrier layers are functional films, which can be applied to polymeric substrates with the objective of enhancing their end-use properties. For food packaging applications, the packaging material is required to preserve packaged food stuffs and protect them from a variety of environmental influences, particularly moisture and oxygen ingress and UV radiation. Aluminum metallized films are widely used for this purpose. More recently, transparent barrier coatings based on aluminum oxide or silicon oxide have been introduced in order to fulfill requirements such as product visibility, microwaveability or retortability. With the demand for transparent barrier films for low-cost packaging applications growing, the use of high-speed vacuum deposition techniques, such as roll-to-roll metallizers, has become a favorable and powerful tool. In this study, aluminum oxide barrier coatings have been deposited onto biaxially oriented polypropylene and polyethylene terephthalate film substrates via reactive evaporation using an industrial 'boat-type' roll-to-roll metalliser. The coated films have been investigated and compared to uncoated films in terms of barrier properties, surface topography, roughness and surface

energy using scanning electron microscopy, atomic force microscopy and contact angle measurement. Coating to substrate adhesion and coating thickness have been examined via peel tests and transmission electron microscopy, respectively.

Keywords: Aluminum oxide, BOPP, barrier coatings, reactive evaporation, adhesion, surface energy

1. Introduction

Polymer films vacuum coated with a thin layer of evaporated aluminum are a standard component in the composite structure of flexible packaging materials for a variety of food stuffs. These thin coatings with a thickness of a few tens of nanometers [1] are produced on industrial roll-to-roll vacuum web coaters, generally referred to as metallizers. The machines predominantly use restively heated evaporation boats and can coat films of a width of 4.45 m at speeds up to 1000 m/min [2, 3]. The main purpose of applying these thin layers is to confer barrier properties to the polymer films, which on their own generally do not act as good barriers, and thus create a functional packaging material. The impermeability of the packaging material to vapors and gases such as water, oxygen, carbon dioxide and aromas (either going into or coming from the product) is an essential design consideration for the longevity of the packaged food product and hence key to successful food packaging. In recent years, transparent barrier coatings, such as aluminum oxide or silicon oxide (usually referred to as AlO_x and SiO_x as the exact stoichiometry is not generally measured) have been gaining interest. When applied onto polymer films, these barrier coatings bring additional advantages over opaque metallized films in that they offer product visibility, microwaveability/retortability and are also suitable for passing through metal detectors, whilst still providing the barrier levels required. With the transparent barrier flexible packaging market growing worldwide at a rate of 10 to 15 % per year [2], the use of vacuum deposition techniques to produce transparent barrier layers has become very attractive. Products such as ethylene vinyl alcohol copolymer (EVOH) coated and coextruded barrier films and polyvinylidene chloride (PVdC) atmospheric coated polymer films conventionally tend to dominate this market [4]. However, vacuum deposited thin barrier coatings only require a small fraction of the thickness of these polymer based barrier layers, i.e. their thickness is three orders of magnitude less, whilst still producing similar barrier properties. This can potentially provide vast economic and environmental benefits in terms of raw material

consumption and the associated costs. Using and modifying a standard 'boat type' roll-to-roll metalliser to deposit transparent barrier coatings has been an aspiration for many years [5-10]. The injection of oxygen into the aluminum vapor stream in the evaporation zone results in the deposition of a transparent aluminum oxide layer, which can give good barrier properties, when the process and its conditions are controlled appropriately. When using polyethylene terephthalate (PET) base film, this process produces consistent barrier performance with the reactively evaporated aluminum oxide. However, considering the low profit margins within the packaging market, the associated cost of the base substrate also plays a major part and commodity biaxially oriented polypropylene (BOPP) films still remain at a lower cost level than PET. The barrier levels of aluminum oxide coated BOPP, though, are heavily affected by the plain film surface characteristics and thus the growth conditions created for the depositing thin film. As will be shown, the surface characteristics of standard packaging grade BOPP films can vary significantly. Therefore, this paper reports the characterization of plain film surface properties, such as surface energy, roughness and topography and relates the findings to the barrier levels obtained after AlO_x coating. Additionally, coating adhesion and coating surface energy, important parameters for further conversion of vacuum coated films, and coating thickness have been assessed using peel tests, contact angle measurement and transmission electron microscopy, respectively

2. Experimental

2.1. Substrate materials

Various packaging grade BOPP films and a PET base film (all corona treated in-house by the film producers), as well as a BOPP film coextruded with a special high surface energy polymer as a skin layer ('UHB', produced by Brückner Maschinenbau GmbH & Co. KG, Siegsdorf, Germany) were coated with an aluminum oxide barrier layer. The coatings were applied to the corona treated side of each film and the high surface energy polymer skin layer, respectively. All standard packaging grade BOPP films used consist of a three layer

coextruded structure with a homopolymer core and either co- or terpolymer skin layers on each side in order to obtain a heat-sealable film. These skin layers also contain additives such as antiblock particles (up to several μm in diameter, typically consisting of silica), which ensure good film processing and converting characteristics. However, they are also known to negatively impact the barrier properties of vacuum deposited coatings. In contrast to the standard packaging grade BOPP films, the BOPP film with the special polymer skin layer consists of a five layer coextruded structure, with no antiblock particles added to the high surface energy polymer skin layer [11]. The PET film coated as a reference material is a monolayer film, with antiblock particles dispersed throughout the single layer. Furthermore, all films contain a variety of additives to stabilize the polymer film and guarantee optimized film handling and end-use properties. Exact film compositions are, however, commercially sensitive information not made available by the individual film producers.

2.2. Coating process

The polymer films were coated via reactive thermal evaporation using a Bobst Manchester Ltd. (formerly General Vacuum Equipment Ltd.) General K4000 vacuum metallizer with an AlO_x coating system installed. The K4000 roll-to-roll metallizer can handle webs up to 2450 mm wide and the AlO_x coating process was performed at web speeds up to 840 m/min. For the films coated here, the web width varied between 1000 mm and 1650 mm and samples were generally taken from the center of the web. The vacuum coater has a deposition source consisting of resistively heated evaporation boats (standard intermetallic composite) onto which aluminum is continuously fed in the form of a wire. Oxygen is introduced into the aluminum vapor stream in order to produce a transparent aluminum oxide coating and a special optical monitor beam and closed loop control system is used to achieve consistent optical properties of the coated film across the web width and length. The pressure during aluminum oxide deposition is of the order of 0.05 Pa. Additionally, in-line plasma pre- and post-treatments were performed using a plasma source with magnetically enhanced water

cooled electrodes. The pressure at the plasma treatment units is kept between 2 and 4 Pa, in order to minimize unintended sputtering from the electrodes. The plasma treatment was performed using power settings and gas recipes previously optimized at Bobst. For this study, other than the plasma treatment conditions, all coating parameters were kept constant to ensure coatings of comparable thickness and stoichiometry.

2.3. Analytical techniques

Barrier properties, in terms of oxygen and water vapor transmission rates (OTR/WVTR), were determined in accordance with ASTM F 1927 and ASTM F 1249/ISO 15106-3 using a Mocon Oxtran 2/20 and Systech Illinois 8001 for oxygen permeation and a Mocon Permatran-W 3/33 and Systech Illinois 7001 for water vapor permeation. Test conditions for OTR were 23 °C and 50 % relative humidity (RH), whilst WVTR is stated for 37.8 °C and a gradient of 90 % RH.

Furthermore, a Zeiss Supra 40VP field emission gun scanning electron microscope (SEM) was used to acquire images of the uncoated and aluminum oxide coated film surfaces at an acceleration voltage of 0.4/0.5 kV. In order to avoid masking any surface detail, no conductive layer was applied to these insulating samples prior to analysis.

The plain film and coating surfaces were additionally analyzed with a WiTec alpha500 and a Veeco DI CP II atomic force microscope (AFM). Pulsed force mode and tapping mode, respectively, were used to acquire roughness data and topography images. All images were corrected by first order line-wise leveling. Root mean square (RMS) and roughness average (R_A) values were calculated from 5 x 5 μm^2 size scans. Therefore, several scans were performed of different areas that did not exhibit antiblock particles in order to obtain an average value and the standard deviation.

The coating to substrate adhesion was assessed using a peel test, as described in further detail in Ref. [12, 13]. This industrial based test is normally applied to examine the adhesion of aluminum metallized films. For this test, an ethylene acrylic acid (EAA) film is bonded to the

coated surface of the polymer film and, after conditioning, the EAA/coating is peeled off at a peel-off angle of 180°.

The surface energy of the uncoated films and the AlO_x coating surface energy were investigated by means of contact angle measurement via the sessile drop method. Contact angles for three different test fluids (water, diiodomethane and ethylene glycol) were measured with a Krüss MobileDrop system and DSAII software. When curve fitting and measurement of contact angles was not possible with the Krüss system, the acquired images were analyzed using a drop shape analysis plugin for ImageJ [14]. These angles were then used to calculate the surface energies according to the Owens-Wendt-Rabel-Kaelble approach [15-17]. Throughout this investigation, sample swatches were stored under ambient conditions.

A FEI Tecnai 12 Biotwin transmission electron microscope (TEM) at a 100 kV acceleration voltage was used to acquire images of the AlO_x layer for coating thickness evaluation after embedding and ultra-microtome sectioning.

3. Results and discussion

3.1. Barrier performance

The barrier performance obtained for the plain BOPP films and the AlO_x coated films is summarized in *Table I*. Also listed in this table are the results for a PET reference film and the results following different plasma treatments. These values were used to determine the barrier improvement factor (BIF) for each transmission rate (i.e. transmission rate ratio of uncoated to coated film), which is a quality indicator commonly used to characterize the effect of vacuum deposited barrier coatings. The results presented in *Table I* allow the BOPP films to be rated with respect to their barrier performance after AlO_x coating:

- BOPP A – poor performing polymer
- BOPP B – standard performing polymer

- BOPP C – standard performing polymer with improved oxygen barrier
- BOPP D – BOPP with special polymer skin layer

As mentioned in section 1, AlO_x coated standard packaging grade PET delivers consistent barrier properties, typically around or less than 1 cm³(STP)/(m² d bar) and 1 g/(m² d). This can be seen from the OTR and WVTR values in *Table I*, which are both around 0.5 cm³(STP)/(m² d bar) and 0.5 g/(m² d), respectively, for the PET reference sample. However, when coating standard packaging grade BOPP films with reactively evaporated AlO_x, the barrier performance can vary to a large extent and appears to be strongly affected by the individual base material itself. BOPP, in contrast to PET, is a non-polar polymer with a completely different surface chemistry, which can have a large impact on coating nucleation and growth [18]. For AlO_x coated BOPP A for example, the OTR was very inconsistent and the application of plasma treatment did not appear to bring improvement. None of the trials performed resulted in a clear enhancement of the oxygen barrier down to levels below 100 cm³(STP)/(m² d bar), which would be comparable to aluminum metallized BOPP (see for example barrier performance of metallized BOPP B in *Table I*, an OTR value < 100 cm³(STP)/(m² d bar) is generally guaranteed in a datasheet for metallized standard BOPP film). BOPP C, in contrast, delivered acceptable (e.g. < 100 cm³(STP)/(m² d bar) oxygen barrier performance even without any in-line plasma treatment. With the application of pre- and post-treatment an OTR of 26.68 ± 3.07 cm³(STP)/(m² d bar) was achieved for this film. In the case of BOPP D, which is coextruded with a special high surface energy polymer skin layer in order to enhance barrier performance after coating, remarkable barrier improvement for OTR (and WVTR) could be obtained by applying the AlO_x layer (refer to *Table I*). Even without any in-line treatment the OTR (and WVTR) improved significantly, due to the different surface chemistry of the skin layer, which enhances AlO_x nucleation/growth and consequently the coating structure.

The OTR values for both BOPP B and C clearly revealed an improvement in barrier levels obtained when in-line plasma pre- and post-treatments were applied. Pre-treatment improves barrier by chemical modification of the plain film surface, which enhances coating nucleation/growth conditions and hence affects the final coating structure in terms of coating density/porosity [19]. During this chemical modification, functional groups are incorporated into the film surface, which can act as nucleation sites for the depositing coating [12, 20]. Furthermore, plasma treatment is generally accompanied by a cleaning effect, during which low molecular weight species loosely bonded to the film surface are removed through bombardment with energetic plasma species [2]. Bichler and coworkers [21] showed an improvement of the oxygen barrier properties of AlO_x coated BOPP film (electron beam evaporation) following oxygen plasma pre-treatment. They attributed this, though, to the smoothing of the polymer surface induced by the plasma treatment, resulting in the homogeneous growth of the coating. However, as will be shown in section 3.2, we did not find any difference in surface roughness between the plain and AlO_x coated film and hence exclude a smoothing effect of the plasma pre-treatment. The bombardment of the coating during post-treatment can result in a densification of the outermost atomic layers of the coating, which may protect the AlO_x layer and reduce oxygen permeation. Overall, though, these barrier results suggest that barrier performance of AlO_x coated BOPP is very much base film dependent. Possible reasons for the barrier differences between the standard packaging grade BOPP films A, B and C will be discussed along with the results of the SEM and AFM investigations in section 3.2.

For BOPP D, the improvement of OTR by the AlO_x coating (compared to the AlO_x coating on the 'standard' BOPP films) is additionally due to the fact that the 'high surface energy' skin layer itself has a better oxygen barrier than BOPP, as can be seen from the enhanced plain film oxygen barrier performance (refer to *Table I*). As described by Jamieson and Windle [22] and also Beu and Mercea [23], applying a thin and less permeable coating (e.g. polymer layer)

to the polymer film prior to metallization (or in our case AlO_x coating) can improve barrier performance in the case of a defect driven permeation through the inorganic coating due to a reduction of the concentration gradient in the polymer in the vicinity of the defects. This has also been further discussed and explored by Langowski [24].

When investigating the WVTR of the AlO_x coated standard packaging BOPP films, it is clear that, with the exception of BOPP D following pre- and post-treatments, no true moisture barrier improvement was obtained in the trials conducted, i.e., the BIF values are around ≈ 1. An acceptable water barrier level would be less than 1 g/(m² d), i.e. similar to AlO_x coated PET. That good oxygen barrier has been achieved whilst still lacking water barrier improvement, indicates that oxygen and moisture permeation through inorganic barrier layers are dominated by different mechanisms [25-28]. However, plain BOPP film already has an inherently good water barrier compared to plain PET (see *Table I*). For BOPP D, the data in Table I also shows the importance of in-line plasma pre-treatment for obtaining a water barrier performance of less than 1 g/(m² d) for the AlO_x coated film. Once again, the improvement of WVTR with plasma pre-treatment is attributed to the chemical modification and cleaning induced by the plasma treatment. It is assumed that any low molecular weight material on top of the high surface energy polymer skin layer (presumably transferred from the reverse side of the film) is removed by the plasma and thus cannot compromise the depositing coating. This presumably results, along with the functional groups created on the treated film surface, in a better nucleation of the coating and therefore a denser structure exhibiting less defects with a size of a few nm down to the sub-nm range (referred to as microscopic defects [24] or nano-defects [29]) that would predominantly affect water vapor permeation.

3.2. Surface topography and roughness

Due to the large variation of barrier properties obtained for AlO_x coated standard packaging grade BOPP films, the surface topography of the plain BOPP films and AlO_x coated samples

was investigated further at a range of resolutions, using optical microscopy, SEM imaging and finally AFM analysis on 5 x 5 µm² scans.

Light microscopy analysis (no images shown) and SEM analysis (see Fig. 1) revealed major differences between BOPP A, B and C, particularly in terms of the size and density distribution of the antiblock particles present on the film surface. Antiblock particles consist of inorganic materials, typically silica, and are added to the outer layers of the coextruded BOPP film in order to ease film handling during processing. They protrude from the film surface and thus reduce contact area by separating the individual film layers in the rolls of film [30]. Whilst BOPP A and B showed a large number of small (sub µm size) antiblock particles, BOPP C featured fewer but substantially larger antiblock particles (diameter > 1 µm). The damage seen on BOPP A (Fig. 1, left image, center) was created by an antiblock particle dislocating from the film surface. This is a common phenomenon for BOPP films, where the antiblock particles are added to the outer skin layers only and thus are less incorporated into the film, and frequently happens during film conversion and winding. In contrast to all these standard BOPP films, BOPP D does not contain any antiblock particles in its special polymer skin layer. All three standard BOPP films exhibited a 'granular' or 'orange-peel' surface structure, which is a typical characteristic of BOPP films, however, with major individual differences. On BOPP B the grains were a lot larger and more pronounced than on BOPP A and C. In addition to that, another key difference between BOPP A and B/C was seen, in that plain BOPP A was covered in defects shaped like small craters or 'dimples' (see Fig. 1, left image) with diameters of 100 nm to several 100 nm (measured via AFM). These defects were originally assumed to be caused by micro-arcs appearing during corona treatment at the film production site [31]. However, with our more recent investigations we could exclude corona treatment as a potential source of the defects and now focus on the heat setting/thermo fixation applied to BOPP films after the orientation process in order to stabilize the film and prevent unintentional shrinkage. The authors suspect that during this re-

heating process, volatile components within the film surface flash evaporate off and consequently leave crater shaped defects.

When analyzing the AlO_x coated films, it was found that in all cases (BOPP films and also PET reference) the AlO_x coating reproduced the underlying plain film surface topography and showed a similar 'grainy' structure with the individual film characteristics as discussed for the plain BOPP film surfaces. For BOPP A, the AlO_x coating also seemed to recreate the described dimples/craters as pores in the coating and, furthermore, showed irregularities in coating thickness (see Fig. 2). In contrast to that, AlO_x coated BOPP B and C had a very 'regular' surface appearance and did not reveal variations in coating thickness or pores. Based on this observation, the pores in the coating on BOPP A are assumed to act as pathways of unhindered permeation for oxygen, therefore inducing the low oxygen barrier performance of this film after AlO_x coating (refer to *Table I*). For BOPP D (no SEM images shown), the plain as well as the AlO_x coated film surface showed a very smooth surface appearance with no antiblock particles.

The AFM analysis of the plain films and AlO_x coated surfaces confirmed the results of the SEM investigations and revealed the same 'grainy' structures and other surface features (refer to Fig. 3 for AFM images of plain BOPP films). For example, craters/dimples and pores were again detected by the AFM examinations of plain and AlO_x coated BOPP film A, respectively. The SEM and AFM investigations show that the plain film surface and its specific characteristics, such as defects, play an important role in determining the barrier levels obtained after AlO_x coating. For the samples investigated here, the plain film surface defects (dimples/craters) appear to be the main cause for the vast differences in OTR values obtained for BOPP A in contrast to B and C. The AFM analysis was used to collect further information about the surface roughness of the uncoated and coated polymer films in terms of root mean square and roughness average, which have been summarized in *Table II*. Plain and AlO_x coated PET showed the lowest surface roughness, with average RMS values of 1.6 nm

and 1.8 nm, respectively, whilst BOPP B gave the highest roughness values. BOPP D with its special polymer skin layer showed a slightly higher surface roughness than PET, but was still smoother than all the analyzed standard packaging grade BOPP films. BOPP A and C revealed the same surface roughness values, despite the dimples/craters present in the surface of BOPP A. For the plain PET and BOPP films, the surface roughness values measured in this study are in agreement with results obtained by Benmalek and Dunlop [32] and Deng et al. [18]. When investigating the AlO_x coated samples, the roughness data obtained was very similar to the plain films and no impact of pre- or post-treatment on the roughness of the AlO_x layer was observed. For each film type, plain and AlO_x coated film exhibited virtually identical surface roughness values, which again indicates that the thin AlO_x layer reproduces the underlying surface roughness and structure as seen in the SEM investigation. Deng et al. [18], who used electron beam evaporation to deposit AlO_x layers onto PET and polypropylene, found that this was only the case for PET, whilst for polypropylene the 10 nm AlO_x layer showed an increased roughness compared to the plain film (the thickness of the coatings investigated in our study is identical, see section 3.4, however a lower scan size of 1 x 1 μm^2 was used by Deng et al. [18]). Therefore, they hypothesized an island growth mechanisms for the AlO_x layer on polypropylene and a layer-by-layer growth mechanism on PET. The work presented here, however, suggests that there is no difference for BOPP compared to PET, as for each BOPP film type, the plain and AlO_x coated films showed similar/identical surface roughness. Nevertheless, the authors still assume that the AlO_x layer grows in a different manner (nanostructure of the coating) on BOPP than it does on PET, due to the different surface chemistry, and this contributes to the different barrier properties. This nanostructure of the coating does, however not affect the roughness of the AlO_x coating, as measured by AFM, i.e. it is beyond the resolution of this analytical technique at the chosen scan size.

Not taking BOPP A into account, the roughness data may suggest that a smoother surface results in better barrier properties after AlO_x coating. In the case of BOPP D and PET, we however assume that the barrier improvement is caused by the change in surface chemistry (see section 3.3) whilst for BOPP B and C there are further differences (such as the antiblock particle size and distribution density) that are known to have an impact on barrier properties. Antiblock particles protruding up to several microns from the film surface will quite likely result in defects in the coating. BOPP B showed a larger number of micron and submicron size antiblock particles, whilst BOPP C showed substantially larger particles and a lesser amount of smaller particles. This may potentially have a large impact on the barrier properties after AlO_x coating, as other researchers state that "many small holes in a barrier layer are much more effective in compromising the system barrier properties than a few large holes with the same total area" [33].

3.3. Surface chemistry

The plain polymer films were further characterized in terms of surface chemistry via contact angle measurement for surface energy determination. This technique can be regarded as an indirect method to assess information about the chemical composition of the different substrate film surfaces. As can be seen from the results presented in *Table III*, the total surface energies of BOPP B and C with values around 36.5 mN/m are slightly lower than for BOPP A, which shows an average surface energy of 38.0 mN/m. All surface energies of the corona treated standard packaging grade BOPP films are, though, typical levels to be expected for industrially corona treated BOPP film [34, 35]. It is, however, well known that corona treated polypropylene film undergoes an ageing process [34, 36]. This thermodynamically driven process causes the polymer surface to revert towards its initial more hydrophobic state and is explained by mechanisms including reorientation of the functional groups created towards the bulk polymer; migration of mobile short polymer chains (low-molecular-weight material created by the treatment) to the polymer surface; or diffusion of additives to the film surface,

and its extent depends strongly on ambient conditions [20, 37]. It may, therefore, well be that differences in the polarity of the film surfaces are present, but are not detected due to the nature of the contact angle measurement, which only probes the outermost atomic layers. Furthermore, the films are coated in vacuum and in this environment volatile components may desorb from and leave the film surface more readily due to the lower vapor pressure. Thus, these components may interfere with the contact angle measurements conducted under atmospheric conditions, but have less impact for the depositing coating in vacuum. In order to further characterize the films and detect possible differences, the exact chemical composition of the plain BOPP films needs to be studied using X-ray photoelectron spectroscopy (XPS) analysis.

The total surface energies of BOPP D, the film with the modified skin layer, and PET are higher compared to the standard BOPP films, which is due to a higher dispersive surface energy component. This difference is caused by the different chemical surface composition of these films and it is assumed that this surface chemistry creates better nucleation conditions for the depositing AlO_x layer, therefore improving growth and structure/density of the coating, which in turn enhances the barrier properties. The surface energy of BOPP D measured in this study is lower than expected, based on published data [38]. However, it has to be noted that the high surface energy polymer skin layer is in contact with the low surface energy reverse side of BOPP D (a polypropylene copolymer) when stored in roll form and material may be transferred from the reverse onto the special skin layer, thus reducing the surface energy measured. It is also worthwhile mentioning that, whilst the surface energy measured using dyne pens according to ASTM D-2578 was in good agreement with the results obtained via contact angle measurement and the calculation approach used for BOPP A to D, there was a strong discrepancy for the surface of the corona treated PET film. However, different techniques (i.e. test fluids, calculation methods) will result in different surface energies [39].

3.4. Coating thickness

In order to determine the thickness of the reactively evaporated AlO_x layers, film samples were embedded in an epoxy resin, cross-sectioned with an ultramicrotome and subsequently examined using TEM. Fig. 4 shows representative TEM cross-section images for AlO_x coated BOPP C at two different magnification levels. For standard BOPP films, TEM revealed the typical three layer structure with a core layer surrounded by a skin layer on each side. One of the skin layers, i.e. the skin layer that is coated with AlO_x, can be clearly seen in the lower magnification TEM image (Fig. 4 A) and reveals a thickness of less than 0.5 µm. Here, it is also observable that the AlO_x layer fractures during TEM sample preparation, caused by the compression of the microtoming process and the different elastic properties of the BOPP polymer, the embedding medium and the ceramic AlO_x layer. In all cases, the thickness of the AlO_x barrier layer was determined to be between 9 and 11 nm (refer to Fig. 4 B) independent of the barrier performance. This thickness is approximately only one fourth of the thickness of an aluminum barrier layer on a standard metallized film with an optical density of 2.5 [1], which is used in food packaging applications. It was also attempted to investigate the structure of the coating using the TEM cross-section images. However, no structural differences were visible between the AlO_x coating on the various BOPP films and PET film at the resolution level provided by TEM analysis. It is therefore concluded that the nanostructure and potential differences of the approximately 10 nm thin AlO_x coatings cannot be resolved using TEM analysis of cross-sections. The thickness in our study is similar to aluminum oxide barrier layers deposited by other researchers using PVD processes [40, 41], who found that effective barrier properties can be obtained at such a coating thickness. However, it disagrees with Kelly [6], who stated that below 15 nm coating thickness the reactively evaporated AlO_x layer is discontinuous and barrier properties are impaired.

3.5. Coating adhesion

The AlO_x coated samples were further investigated to gain information about coating to substrate adhesion, which is an important aspect for the conversion of vacuum coated films. A 180 degree peel test was used in this investigation and the peel force values obtained are summarized in *Table IV*. In our previous work [31] we have shown that for AlO_x coated BOPP very high peel force values where obtained, independent of the plasma treatment applied and also independent of the barrier performance, thus indicating that insufficient barrier properties are not related to poor adhesion. This was also found for the additional BOPP films investigated in this study. In all cases, infra-red spectroscopy of the peeled-off EAA layer proved that cohesive failure had occurred within the polymer substrate during the peel test. Based on the probing depth of the analytical technique used for polymer identification, it was concluded that in addition to the AlO_x coating, the skin layer of the coextruded BOPP films was also peeled off with the EAA film. Since adhesion failure in a multilayer system generally occurs at the weakest point [42], it can be assumed that the adhesion of the AlO_x coating to the BOPP film exceeds the values measured. *Table IV* also contains reference values for metallized BOPP A and B, which are a lot lower than the forces obtained for their AlO_x coated opponents and, furthermore, did not show removal of the BOPP skin layer along with the metal coating. Peel tests were additionally carried out for the AlO_x coated PET and the AlO_x coated 5 layer BOPP film coextruded with a different polymer as skin layer. Also, for the latter film, the skin layer was removed during all peel tests. For AlO_x coated PET, it was, though, not possible to peel off the AlO_x layer. Here the EAA film stretched until it tore at values around 6 to 7 N/(15 mm) without removing any AlO_x or parts of the PET film. This is attributed to the PET substrate being a single layer and not a coextruded film. Due to the high intrinsic strength of this single layer material, no cohesive failure within the PET film can occur. Indeed, in the case of PET, the EAA peel test is known to be reaching its limits [13].

3.6. AlO_x surface energy

In addition to coating to substrate adhesion, coating surface energy is a further important factor to be considered for conversion processes of the vacuum coated films, such as printing or laminating on top of the barrier layer. These process steps require a high surface energy as this usually results in better wetting of inks or the adhesives used for lamination. Good wetting, in general, is the first step towards good adhesion. The AlO_x coated films were investigated using contact angle measurement to calculate their surface energy. Samples were stored under ambient conditions without precise control of environmental parameters as this is seen as a more realistic approximation to the storage conditions of industrial film rolls. We have previously published the initial results of this investigation [31] and are now presenting the long term behavior of the samples examined. The measurements were carried out over an extended period of approximately 700 days and results are depicted as a function of time in Fig. 5. For AlO_x coated BOPP A, which was initially analyzed on the day of coating, a rapid decrease of the total surface energy from a start value of 57.0 ± 0.9 mN/m is visible for the first few days after coating, followed by a further decay at a lower rate until around 175 days of age. From this time onwards, there was still a measurable, but very slow, decline with current values at around 40 mN/m. BOPP D behaved nearly identically to BOPP A and also BOPP C showed similar behavior, although the average AlO_x surface energy was somewhat higher than for the other films. However, over extended time periods, AlO_x coated BOPP C appears to approach surface energy values similar to the other two AlO_x coated BOPP films. For comparison, Fig. 5 also contains surface energies obtained on AlO_x coated PET. These values are considerably higher (63 to 66 mN/m) and also only reveal a marginal decrease with time. As discussed in more detail in our earlier work [31] this drop of coating surface energy is caused by the transfer of polymeric material and film additives from the reverse of the polymer film onto the fresh coating and also the migration through the coating via defects. This happens as soon as the coated film is wound into a roll and a contact is established

between the fresh coating and the reverse side of the polymer film. Consequently, it is inevitable for roll to roll coating processes. In the case of all BOPP films, including BOPP D with a different polymer as skin layer, the reverse side is a polypropylene surface, either a co- or terpolymer. Hence, the three BOPP films behave very similarly, in contrast to the AlO_x coated PET. Differences between PET and BOPP in terms of the surface energy decay characteristics of the AlO_x coated side can be explained by the difference in glass transition temperature (T_g) of the two polymers. BOPP at ambient temperature will be above its T_g (in the range of 0 to 10 °C [43] for isotactic PP) and consequently all amorphous parts will be in a rubbery state. In this state, polymer chains and fragments are more flexible and mobile. In contrast, PET has a higher T_g (69 to 115 °C [43]). Thus, in PET the oligomers and polymer chains in the amorphous regions are in the glassy state at ambient temperature and are less mobile; it is therefore argued that less migration will occur. In addition to that, fewer film additives are required during PET film production. XPS surface analysis of the AlO_x coated BOPP and PET films in this study confirmed the presence of carbon based material as well as residues of film additives, such as acid scavengers (for BOPP), on the AlO_x coating, assumed to have come from contact with the reverse side of the film. Furthermore, there was a larger amount of carbon based contamination on AlO_x coated BOPP than on AlO_x coated PET, which is in good agreement with the surface energy being higher for the AlO_x coating on PET compared to any type of BOPP.

4. Summary and conclusions

Barrier properties of packaging grade PET and BOPP films, coated with aluminum oxide via reactive thermal evaporation, are strongly affected by the surface characteristics of the plain film, such as surface defects and surface chemistry. These parameters have a large impact onto the aluminum oxide coating nucleation, growth and structure and not only vary to a large extent between the different polymer film types, but can also change significantly within one

substrate type, as has been shown here for standard packaging grade BOPP films. The barrier levels obtained for PET films coated with reactively evaporated aluminum oxide are consistent and reliably achieved. In contrast to that, though, AlO_x coated BOPP films exhibit significant differences in their barrier performance, depending on the individual substrate. Substrate surface defects, such as the craters/dimples found on BOPP A appeared to play an important role in compromising barrier properties. These defects were found to be reproduced as pores in the AlO_x coating, thus acting as permeation pathway for oxygen and increasing the measured transmission rates for BOPP A compared to B and C. Furthermore, the standard packaging grade BOPP films also featured considerable differences in the antiblock particle size and density, which can potentially affect the size and number of defects in the AlO_x layer, and therefore is of great importance to the barrier levels that can be achieved. The surface energy determination for the plain standard BOPP films could not explain the differences seen in barrier performance after AlO_x coating, as all corona treated standard packaging grade BOPP films showed a similar value. For the PET film, as well as the BOPP film coextruded with a special skin layer, the surface energy was higher than for the corona treated BOPP films, due to the different surface chemistry. With respect to surface chemistry, XPS analysis of all plain films is needed in order to investigate compositional differences, which, in the case of the corona treated BOPP films, were potentially not detected using contact angle measurement. TEM analysis indicated an average thickness of 10 nm for all AlO_x coatings, but could, unfortunately, not reveal any structural differences between the individual coatings on the BOPP films and PET reference film. For all films a very high coating to substrate adhesion was observed, which resulted in cohesive failure of the substrate occurring during peel tests of the AlO_x coated BOPP films. Therefore, poor barrier performance is not related to insufficient adhesion. An important result is that the use of a high surface energy polymer skin layer, which can be coextruded with the BOPP film, significantly helps to improve the

oxygen as well as water vapor barrier performance of AlO_x coated BOPP film and thus to obtain barrier levels comparable to AlO_x coated PET.

Acknowledgements

The authors would like to thank Bobst Manchester Ltd. (Heywood, United Kingdom) for providing an industrial trial platform and, moreover, film producers and customers including Brückner Maschinenbau GmbH & Co.KG (Siegsdorf, Germany) for supplying base films. Additionally, we are grateful to Innovia Films Ltd. (Wigton, United Kingdom) for being able to use their analytical facilities, the Fraunhofer Institute for Process Engineering and Packaging IVV (Freising, Germany) for giving access to their AFM and Dr. Aleksandr Mironov of the electron microscope facility in the Faculty of Life Sciences of the University of Manchester (Manchester, United Kingdom) for his assistance in performing TEM analysis. Furthermore, we thankfully acknowledge Dr. Charles Bishop for his valued comments and input.

References

[1] D.J. McClure, N. Copeland, AIMCAL 2010 Fall Technical Conference, AIMCAL, 2010.

[2] C.A. Bishop, Roll-to-roll vacuum deposition of barrier coatings, Scrivener, Salem, 2010.

[3] R. Ludwig, R. Kulka, E. Josephson, Proc. IEEE 93 (2005) 1483-1490.

[4] The future of transparent barrier films to 2011, Pira International Ltd., Leatherhead, 2006.

[5] R.S.A. Kelly, in: Proceedings of the 36th Annual Technical Conference of the Society of Vacuum Coaters (1993) pp. 312-316.

[6] R.S.A. Kelly, in: Proceedings of the 37th Annual Technical Conference of the Society of Vacuum Coaters (1994) pp. 144-148.

[7] S. Schiller, M. Neumann, H. Morgner, N. Schiller, in: Proceedings of 7th International Conference on Vacuum Web Coating (1993) pp. 194-219.

[8] S. Schiller, M. Neumann, H. Morgner, N. Schiller, in: Proceedings of the 37th Annual Technical Conference of the Society of Vacuum Coaters (1994) pp. 203-210.

[9] N. Schiller, S. Straach, S. Günther, A.L. Quiceno, A.G. Contreras, R. Ludwig, G. Hoffmann, AIMCAL 2008 Fall Technical Conference, AIMCAL, 2008.

[10] S. Günther, S. Straach, N. Schiller, A.L. Quiceno, A.G. Contreras, R. Ludwig, G. Hoffmann, in: Proceedings of the 52nd Annual Technical Conference of the Society of Vacuum Coaters (2009) pp. 727-729.

[11] J. Breil, in: J.R. Wagner Jr. (Ed.), Multilayer flexible packaging: technology and applications for the food, personal care and over-the-counter pharmaceutical industries Elsevier, Amsterdam, 2010, pp. 231-237.

[12] H.-C. Langowski, J. Adhes. Sci. Technol. 25 (2011) 223-243.

[13] M. Jesdinszki, C. Struller, N. Rodler, D. Blondin, V. Cassio, E. Kucukpinar, H.-C. Langowski, J. Adhes. Sci. Technol. 26 (2012) 2357-2380.

[14] A.F. Stalder, G. Kulik, D. Sage, L. Barbieri, P. Hoffmann, Colloids Surf. A Physicochem. Eng. Asp. 286 (2006) 92-103.

[15] D.K. Owens, R.C. Wendt, J. Appl. Polym. Sci. 13 (1969) 1741-1747.

[16] W. Rabel, Farbe und Lack 77 (1971) 997-1005.

[17] D.H. Kaelble, J. Adhes. 2 (1970) 66-81.

[18] C.S. Deng, H.E. Assender, F. Dinelli, O.V. Kolosov, G.A.D. Briggs, T. Miyamoto, Y. Tsukahara, J. Polym. Sci. B Polym. Phys. 38 (2000) 3151-3162.

[19] W. Decker, B. Henry, in: Proceedings of the 45th Annual Technical Conference of the Society of Vacuum Coaters (2002) pp. 492-502.

[20] E.M. Liston, L. Martinu, M.R. Wertheimer, J. Adhes. Sci. Technol. 7 (1993) 1091-1127.

[21] C. Bichler, T. Kerbstadt, H.C. Langowski, U. Moosheimer, Surf. Coat. Technol. 112 (1999) 373-378.

[22] E.H.H. Jamieson, A.H. Windle, J. Mater. Sci. 18 (1983) 64-80.

[23] T.A. Beu, P.V. Mercea, Mater. Chem. Phys. 26 (1990) 309-322.

[24] H.-C. Langowski, in: O.G. Piringer, A.L. Baner (Eds.), Plastic Packaging - Interactions with Food and Pharmaceuticals, Wiley-VCH, Weinheim, 2008, pp. 297-347.

[25] O. Miesbauer, M. Schmidt, H.-C. Langowski, Vakuum in Forschung und Praxis 20 (2008) 32-40.

[26] M. Hanika, H.-C. Langowski, W. Peukert, in: Proceedings of the 46th Annual Technical Conference of the Society of Vacuum Coaters (2003) pp. 592-599.

[27] A.G. Erlat, B.M. Henry, C.R.M. Grovenor, A.G.D. Briggs, R.J. Chater, Y. Tsukahara, J. Phys. Chem. B 108 (2004) 883-890.

[28] Y.G. Tropsha, N.G. Harvey, J. Phys. Chem. B 101 (1997) 2259-2266.

[29] A.P. Roberts, B.M. Henry, A.P. Sutton, C.R.M. Grovenor, G.A.D. Briggs, T. Miyamoto, M. Kano, Y. Tsukahara, M. Yanaka, J. Memb. Sci. 208 (2002) 75-88.

[30] T. Kromminga, G. Van Esche, in: H. Zweifel, R.D. Maier, M. Schiller (Eds.), Plastic Additives Handbook, Carl Hanser, Munich, 2008, pp. 613-628.

[31] C.F. Struller, P.J. Kelly, N.J. Copeland, C.M. Liauw, J. Vac. Sci. Technol. A 30 (2012) 041502.

[32] M. Benmalek, H.M. Dunlop, Surf. Coat. Technol. 76-77 (1995) 821-826.

[33] G. Rossi, M. Nulman, J. Appl. Phys. 74 (1993) 5471-5475.

[34] J.M. Strobel, M. Strobel, C.S. Lyons, C. Dunatov, S.J. Perron J. Adhes. Sci. Technol. 5 (1991) 119-130.

[35] R. Wolf, A.C. Sparavigna, Engineering 2 (2010) 397-402.

[36] M. Strobel, C.S. Lyons, J.M. Strobel, R.S. Kapaun, J. Adhes. Sci. Technol. 6 (1992) 429-443.

[37] F. Garbassi, M. Morra, E. Occhiello, Polymer Surfaces - from Physics to Technology, John Wiley & Sons, Chichester, 1994.

[38] M. Wolf, J. Breil, R. Lund, TAPPI 2008 PLACE Conference, TAPPI, 2008.

[39] M. Zenkiewicz, J. Adhes. Sci. Technol. 15 (2001) 1769-1785.

[40] N. Schiller, H. Morgner, M. Fahland, S. Straach, M. Räbisch, C. Charton, in: Proceedings of the 42nd Annual Technical Conference of the Society of Vacuum Coaters (1999) pp. 392-396.

[41] R.W. Phillips, T. Markantes, C. LeGallee, in: Proceedings of the 36th Annual Technical Conference of the Society of Vacuum Coaters (1993) pp. 293-301.

[42] K.L. Mittal, in: K.L. Mittal (Ed.), Adhesion Measurements of Films and Coatings, VSP, Utrecht, 1995, pp. 1-13.

[43] J.E. Mark, Polymer Data Handbook, second ed., Oxford University Press, New York, 2009.

Table I

Barrier performance (oxygen and water vapor transmission rates) of plain and AlO_x coated BOPP films and PET reference film including barrier improvement factors.

Film type/ base film thickness	In-line Plasma treatment	OTR		WVTR	
		cm^3(STP)/(m^2 d bar)	BIF	g/(m^2 d)	BIF
BOPP A	Plain film	≈ 1600	-	≈ 4	-
30 µm	No	270.50 ± 34.65	6	3.99 ± 0.06	1
	PRE	201.55 ± 24.45	8	3.43 ± 0.35	1.2
	PRE + POST	258.00 ± 18.57	6	3.98 ± 0.30	1
BOPP B	Plain film	≈ 2700	-	≈ 7	-
15 µm	No	475.88 ± 27.45	6	5.78 ± 0.01	1.2
	PRE	118.42 ± 21.70	23	5.47 ± 0.35	1.3
	PRE + POST	79.49 ± 19.58	34	5.89 ± 0.18	1.2
	**Metallized PRE*	*24.65 ± 3.61*	*110*	*0.34 ± 0.03*	*21*
BOPP C	Plain film	≈ 2400	-	≈ 6	-
20 µm	No	47.00 ± 5.35	51	5.89 ± 0.23	1
	PRE	35.33 ± 3.05	68	6.08 ± 0.17	1
	PRE + POST	26.68 ± 3.07	90	4.73 ± 0.07	1.3
BOPP D	Plain film	≈ 500	-	≈ 4.5	-
18 µm	No	0.89 ± 0.01	562	2.19 ± 0.06	2
	PRE	0.83 ± 0.30	602	0.56 ± 0.07	8
	PRE + POST	0.60 ± 0.14	833	0.45 ± 0.11	10
PET	Plain film	≈ 120	-	≈ 40	-
12 µm	PRE + POST	0.54 ± 0.05	222	0.56 ± 0.03	71

**aluminum coating, no AlO_x*

Table II

Surface roughness of plain and AlO_x coated BOPP films and PET reference film (calculated from 5 x 5 µm² AFM scans).

Film	Plasma treatment	RMS	R_A
		nm	nm
BOPP A	Plain film	4.1 ± 0.7	3.3 ± 0.5
	PRE	3.7 ± 0.5	2.9 ± 0.4
	PRE + POST	4.1 ± 0.6	3.2 ± 0.5
BOPP B	Plain film	5.7 ± 1.8	4.5 ± 1.5
	PRE	5.8 ± 0.9	4.6 ± 0.7
	PRE + POST	6.0 ± 0.7	4.8 ± 0.6
BOPP C	Plain film	4.1 ± 0.3	3.2 ± 0.2
	PRE	4.6 ± 0.2	3.6 ± 0.2
	PRE + POST	4.3 ± 0.3	3.4 ± 0.2
BOPP D	Plain film	2.8 ± 0.2	2.2 ± 0.1
	PRE	2.9 ± 0.2	2.3 ± 0.2
	PRE + POST	3.0 ± 0.2	2.4 ± 0.1
PET	Plain film	1.6 ± 0.2	1.2 ± 0.2
	PRE + POST	1.8 ± 0.3	1.4 ± 0.3

Table III

Surface energy results for plain BOPP films and PET reference film. The total surface energy has been split into its polar and dispersive components.

Film	Surface energy mN/m		
	Polar	Dispersive	Total
BOPP A	8.9 ± 0.6	29.1 ± 0.4	38.0 ± 0.4
BOPP B	7.8 ± 0.6	28.6 ± 0.3	36.4 ± 0.4
BOPP C	7.9 ± 0.2	28.7 ± 0.1	36.6 ± 0.2
BOPP D	6.2 ± 1.3	36.2 ± 1.4	42.4 ± 0.3
PET	9.6 ± 0.9	38.6 ± 0.9	48.2 ± 1.3

Table IV

Peel forces obtained for AlO_x coated standard packaging BOPP films (180° peel test, with EAA film).

Film	Plasma treatment	Peel force N/(15 mm)
BOPP A	No	3.16 ± 0.11
	PRE	3.15 ± 0.12
	PRE + POST	3.13 ± 0.08
	**Metallized (PRE)*	0.82 ± 0.04
BOPP B	No	3.46 ± 0.08
	PRE	3.51 ± 0.10
	PRE + POST	3.50 ± 0.16
	**Metallized (PRE)*	0.78 ± 0.03
BOPP C	No	5.05 ± 0.17
	PRE	5.07 ± 0.12
	PRE + POST	5.04 ± 0.14

**aluminum coating, no AlO_x*

List of figure captions

Fig. 1. SEM images of plain film surfaces – left to right: BOPP A, BOPP B, BOPP C.

Fig. 2. SEM image of AlO_x coated BOPP A showing pores in the coating and thickness variations.

Fig. 3. 5 x 5 µm² AFM scans of plain film surfaces – from left to right: BOPP A, BOPP B, BOPP C, BOPP D.

Fig. 4. TEM cross-section images of AlO_x coated BOPP C; A: lower magnification level showing the BOPP skin layer; B: higher magnification level for coating thickness determination.

Fig. 5. Change of AlO_x surface energy with storage time for various AlO_x coated BOPP films and PET reference film.

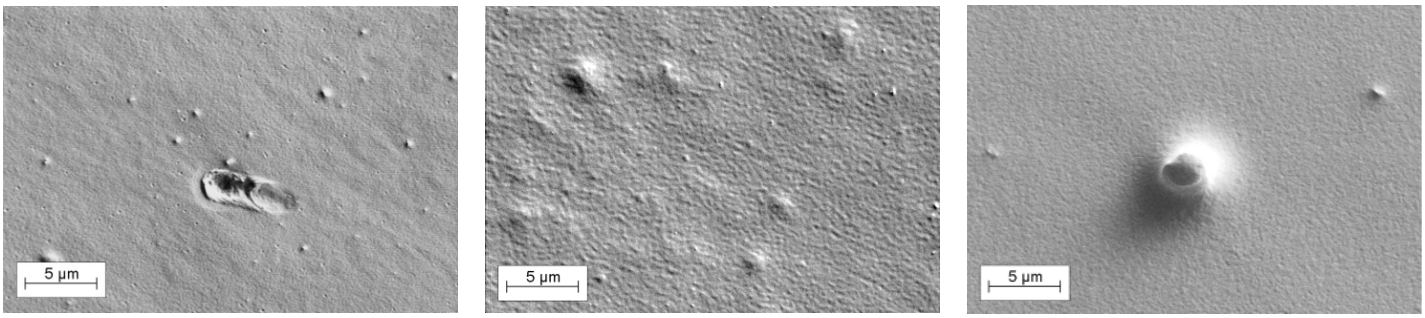

Fig. 1

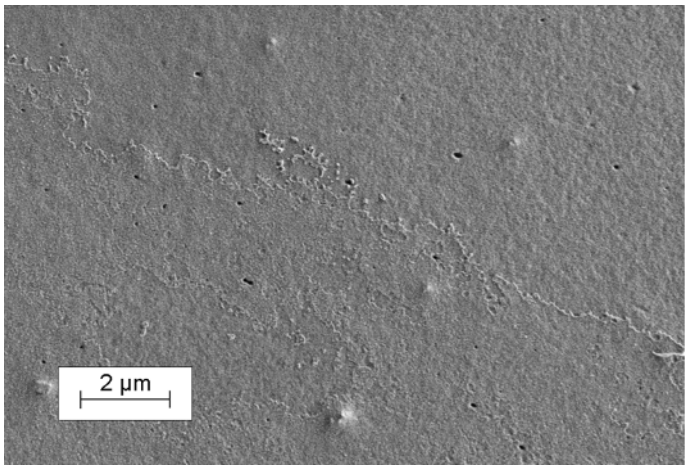

Fig. 2

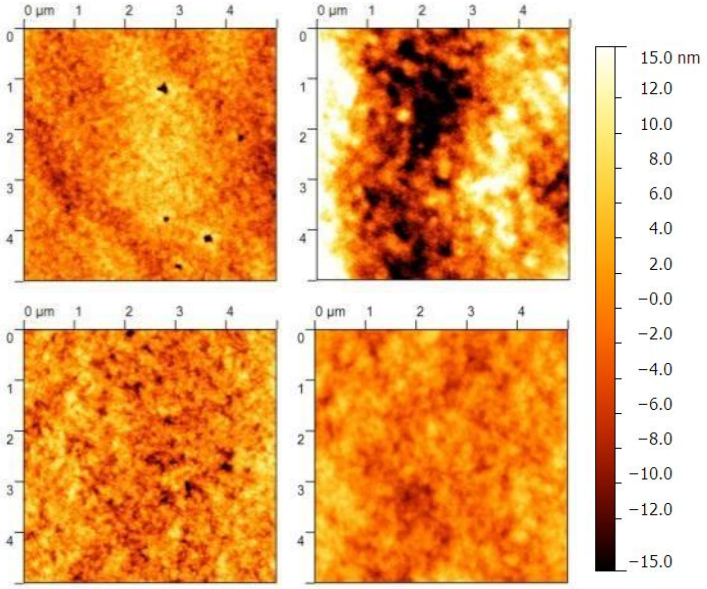

Fig. 3

Color

Fig. 3 to be reproduced in color on the web and in black-and-white in print

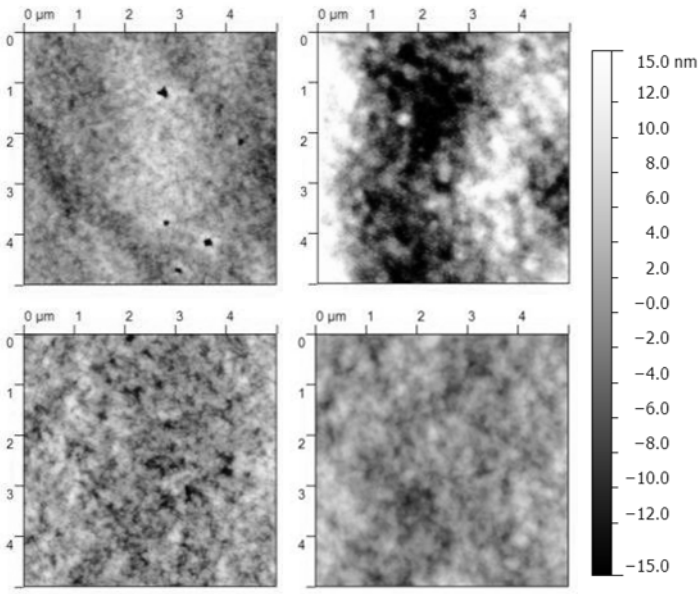

Fig. 3

Black and white

A

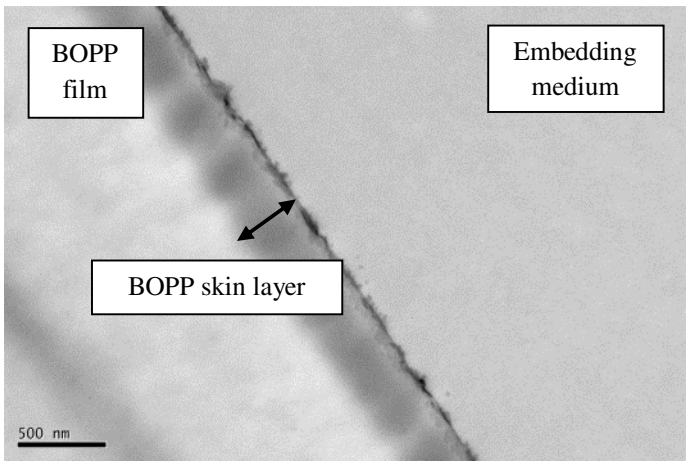
BOPP
film
Embedding
medium
BOPP skin layer
500 nm

B

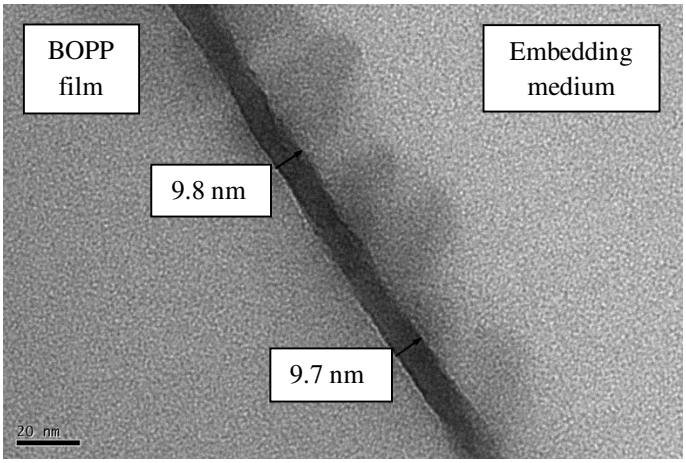
BOPP
film
Embedding
medium
9.8 nm
9.7 nm
20 nm

Fig. 4

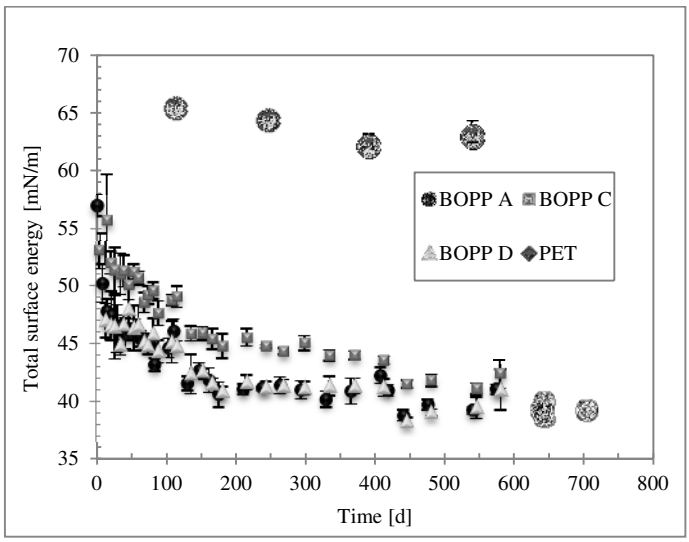
70
65
60
55
50
45
40
35
Total surface energy [mN/m]
0
100
200
300
400
500
600
700
800
Time [d]
BOPP A
BOPP C
BOPP D
PET

Fig. 5